



Controls on the distribution and accumulation of terrigenous organic matter in sediments from the Mississippi and Atchafalaya river margin

Elizabeth S. Gordon*, Miguel A. Goñi

Department of Geological Sciences and Marine Science Program, University of South Carolina, Columbia, SC 29208, United States

Received 21 November 2003; received in revised form 8 April 2004; accepted 30 June 2004

Abstract

Sediment samples from 14 box cores across the Mississippi and Atchafalaya River Margin were examined in order to quantify the magnitude and composition of the OM depositional flux in sediments from a river-dominated margin and identify the fate of terrigenous OM in the study area. Elemental, isotopic, mineral surface area, and terrigenous biomarker analyses suggest that physical sorting of particles across this river-dominated margin controls the chemical composition of sedimentary OM. Sediment accumulation rates in the area ranged from 0.012 to 0.68 cm/year and showed an inverse logarithmic relationship with water depth. Highest organic carbon (OC) content (1.3–1.5%) was observed on the inner shelf (<10 m water depth) and slope (>200 m water depth), with lower OC (0.8%) measured on the outer shelf (10–200 m water depth). Mineral surface area (SA) showed a similar spatial distribution as OC, with the highest values on the inner shelf (average 41 m²/g) and slope (average 54 m²/g), and low SA values (average 23 m²/g) on the outer shelf. Association of OM with minerals and its apparent differential transport across the study area results in the greatest proportion of OM accumulating on the inner shelf (37%), although the slope also plays a significant role in OM accumulation (33%) due to its greater areal extent.

Stable organic carbon isotope ($\delta^{13}\text{C}_{\text{OC}}$) values ranged between -23‰ and -21‰ across the study area, with a slight seaward enrichment. The spatial trend in lignin yields mirrored that of $\delta^{13}\text{C}$, with a substantial decrease in lignin content from 1.8 mg/100 mg OC at inner shelf locations to 0.31 mg/100 mg OC at slope locations. The OC in all sediment samples exhibited more depleted radiocarbon compositions ($\Delta^{14}\text{C}_{\text{OC}}$) than modern values ($>0\text{‰}$), ranging from ca. -200‰ on the inner shelf to ca. -400‰ on the slope. These isotopic and biomarker data indicate that terrigenous OM in the Gulf of Mexico is heterogeneous, composed of at least two sources: lignin-rich, isotopically depleted plant debris and lignin-poor, isotopically enriched soil-derived OM. The plant debris, which is deposited close to shore, composes a small portion of inner shelf sediments. Soil-derived OM is deposited throughout the study area, although it appears to be preferentially transported to deeper regions. The fate of terrigenous OM in the northern Gulf of Mexico appears to be

* Corresponding author. Tel.: +1 803 777 7115; fax: +1 803 777 6610.

E-mail address: gordon@geol.sc.edu (E.S. Gordon).

governed by the hydrodynamic sorting of riverine particles of different compositional character rather than by simple dilution with marine OM.

© 2004 Elsevier B.V. All rights reserved.

Keywords: Terrigenous organic matter; Lignin; Stable carbon isotopes; Marine sediments; Coastal sediments; Gulf of Mexico; Mississippi River; Atchafalaya River

1. Introduction

The burial of organic matter (OM) in margin sediments provides the primary long-term sink for reduced carbon in the ocean (Berner, 1982; Hedges, 1992). River-dominated margins, which receive large quantities of continentally derived sediments and support elevated levels of autochthonous productivity, are quantitatively important sites for OM accumulation and remineralization. Rivers supply enough particulate terrigenous OM to account for all OM deposited in marine sediments (Hedges et al., 1997), so that any additional input from marine carbon would require the recycling of either terrigenous or marine OM in the ocean. Although terrigenous OM is considered to be a recalcitrant pool of carbon and should presumably escape this rapid recycling, current estimates suggest that little terrigenous OM is buried in marine sediments (Hedges and Keil, 1995). Hedges et al. (1997) highlight the “geochemical conundrum” that labile, marine-derived OM apparently persists in the sedimentary record while refractory, land-derived sources comprise a minor proportion of sedimentary OM. The authors contend that either terrigenous OM undergoes efficient recycling in the ocean, or that the current tracers for this material have led to erroneous oceanic OM budgets. The focus of the present manuscript is to address these scenarios by quantifying the magnitude and composition of the OM depositional flux in sediments from a river-dominated margin and identifying the fate of terrigenous OM in the study area.

One difficulty in quantifying oceanic OM budgets is the identification of sedimentary OM sources, particularly whether of marine or terrigenous origin. Early attempts to quantify terrigenous sources of OM in river and coastal sediments in the Gulf of Mexico using stable carbon isotopes (Sackett and Thompson, 1963; Gearing et al., 1977) indicated that terrigenous sources ($\delta^{13}\text{C}$ ca. -26‰) dominated sedimentary OM

close to shore, while marine sources ($\delta^{13}\text{C} = -20\text{‰}$) became predominant offshore. Hedges and Parker (1976) employed a multi-tracer approach towards source determination, using lignin-derived cupric oxide oxidation products in concert with isotopic analyses. The authors concluded that the majority of terrigenous OM in Gulf of Mexico sediments is deposited shoreward of the 100 m isobath, and that land-derived OM delivered to the coastal ocean is a homogenous pool of isotopically depleted, lignin-rich plant fragments. These results formed the basis for the “classic” model for the fate of terrigenous OM in coastal sediments in which isotopically depleted, lignin-rich vascular plant tissues are efficiently diluted with isotopically enriched, lignin-devoid marine OM shoreward of the shelf break. This classic view of negligible terrigenous OM deposited in marine sediments currently persists.

A major assumption in this traditional model of OM sources in the ocean is that the composition of marine sediments can be described by simple two-endmember mixing between marine and terrigenous sources, and that plant fragments accurately represent the terrigenous endmember. Recent research provides evidence that terrigenous OM is heterogeneous in composition, composed of at least two distinct sources, including soils and plant debris (Hedges et al., 1986; Prah et al., 1994; Goñi et al., 1998; Gordon and Goñi, 2003). Despite this recognition, the simplistic view of a homogenous terrigenous endmember often prevails, which has led to an underestimate of the amount of terrigenous OM buried in marine sediments. While plant fragments do appear to compose a portion of the sedimentary mixture in proximal coastal sediments (<10% in deltaic sediments), soil-derived OM composes a significant portion of this material (50–90%; Gordon and Goñi, 2003) in inner and outer shelf sediments. The significant presence of soil-derived OM deposited in marine sediments, which is degraded in nature and

contains lower levels of recognizable biochemicals (such as lignin) than fresh plant fragments, requires a reevaluation of terrigenous OM inputs to the world's oceans.

In this manuscript, we provide additional evidence that terrigenous OM in the Gulf of Mexico has heterogeneous sources (Goñi et al., 1997, 1998; Gordon and Goñi, 2003) and is not confined to the proximal coastal ocean (Bianchi et al., 1997). Our results suggest that the physical processes responsible for the dispersal of sediments in the coastal ocean exert primary control on the composition of sedimentary OM in this river-dominated margin via OM-mineral association and cross-margin transport of different types of OM. In addition, results from this study indicate that the slope plays a more significant role in the accumulation of OM than has previously been appreciated, although the importance of the inner shelf (<10 m water depth) may also have been

underestimated. Finally, a preliminary model of the fate of terrigenous OM on a river-dominated margin is presented, but questions remain regarding the characterization and quantification of this material in marine sediments.

2. Methods

2.1. Study area

The area of study is the Atchafalaya and Mississippi River margin west of the Balize (bird's-foot) delta (Fig. 1). The Mississippi/Atchafalaya River system drains ca. 40% of the continental United States (Fig. 1). Maximum discharge of the Mississippi River (MR) typically occurs between January and June, with peak flow in April. Sediment from the MR (210×10^{12} g year⁻¹, Milliman and Meade, 1983)

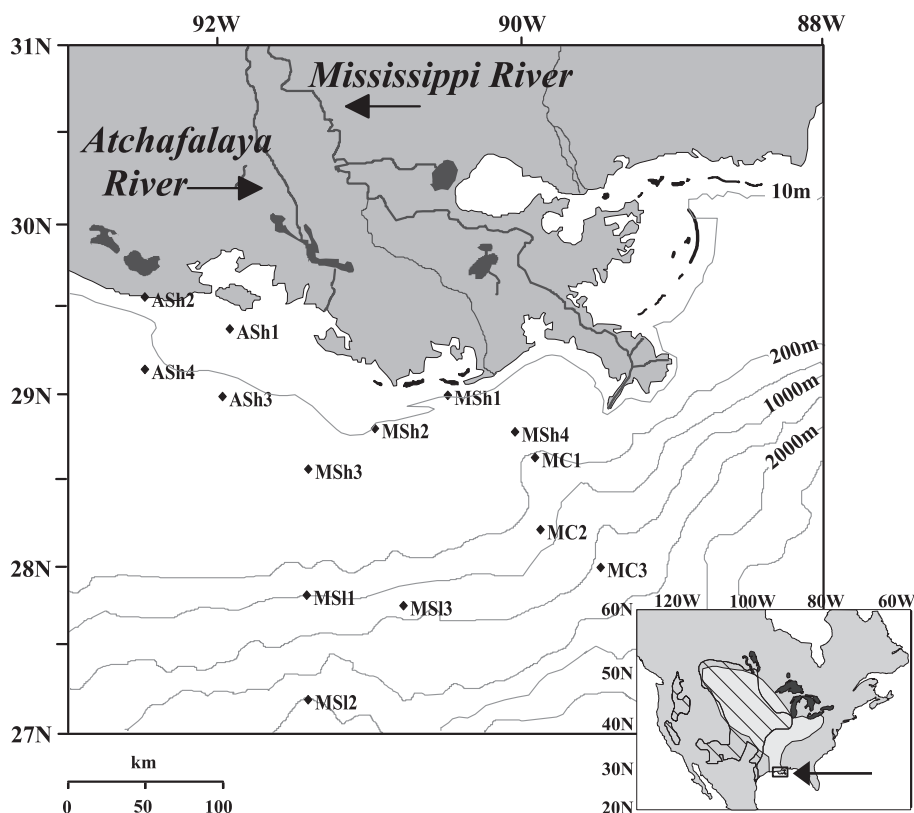


Fig. 1. Map of the study area in the Gulf of Mexico. The light gray region of North America (inset) represents the Mississippi River drainage basin, which overlaps North America's grasslands (hatched area). Sampling locations are indicated by a diamond symbol.

discharges through the bird's-foot delta directly onto the continental shelf within a buoyant sediment plume. Approximately 50% of this discharged material flows to the west of the delta, while the remaining 50% flows to the east (U.S. Army and Corps of Engineers, 1974). In contrast, the Atchafalaya River (AR), its delta located 150 km west of the MR, discharges sediment into a system of shallow (1–4 m) bays before export onto the low-gradient continental shelf. Approximately half of the AR sediment load is transported westward parallel to the coast with the prevailing current to form the Atchafalaya “mud stream” (Wells and Kemp, 1981).

2.2. Sample description

Sediment samples were collected from 14 sites along the Mississippi and Atchafalaya River Margin, within which three regions have been defined for the purposes of this paper: inner shelf (<10 m water depth), outer shelf (10–200 m water depth) and slope (200–2500 m water depth) (Fig. 1; Table 1). Sediments were collected using a 50×50 cm box core in March (ASh1-4, MSh2), May (MSh1, MSh3-4, MC1-3, MSI3), and August (MSI1-2), 1998, and subsampled using a PVC pushcore (6 in. diameter). Each subcore was sampled at 1-cm intervals between 0 and 20 cm, and then sampled

at 2-cm intervals between 20 cm and the core bottom. All samples were refrigerated during transport back to the laboratory, and then stored frozen until analysis. Samples were thawed, sub-sampled, and oven-dried (55 °C). A portion of the dried sediment was ground to pass a 60-mesh (250 μm) sieve prior to elemental, isotopic, and biomarker analyses.

2.3. Analytical methods

2.3.1. Geochronology

Lead-210 geochronology analyses were conducted at Texas A&M University following a modified method of Nittrouer et al. (1979). Leaching of isotopes was achieved through sequential acid treatment, first with HNO₃ and HClO₄, then with HCl. Total activities of ²¹⁰Po, the granddaughter of ²¹⁰Pb, and a yield tracer (²⁰⁹Po) were measured via electroplating and subsequent alpha spectrometry on an EG and G octet detector. Excess ²¹⁰Pb activities used for quantifying sediment accumulation rates were calculated by the difference between total activity and the ²¹⁰Pb activity due to supported decay of the ²²⁶Ra parent. The supported level was determined from the mean activity of samples in cores below the depth of decay-induced, logarithmic decrease in activity. For cores that did not penetrate to the supported depth, supported ²¹⁰Pb activities

Table 1
Sampling locations

Station ID	Date	Latitude (°N)	Longitude (°W)	Water depth (m)	Bottom water salinity (‰)	²¹⁰ Pb accum. rate	
						cm/year	r ²
ASh1	07 Mar 98	29.35	91.91	5	15.9	0.68	0.85
ASh2	07 Mar 98	29.52	92.48	6	11.6	0.55	0.84
ASh3	07 Mar 98	28.95	91.97	22	34.4	0.27	0.86
ASh4	08 Mar 98	29.11	92.48	22	33.7	0.18	0.93
MSh1	07 May 98	28.96	90.48	14	32.0	0.43	0.70
MSh2	06 Mar 98	28.77	90.96	16	32.9	0.091	0.94
MSh3	04 May 98	28.53	91.40	36	35.8	0.33	0.63
MSh4	07 May 98	28.75	90.03	45	36.0	0.056	0.95
MC1	07 May 98	28.60	89.90	365	35.6	0.31	0.92
MC2	06 May 98	28.18	89.87	400	35.3	0.062	0.94
MSI1	16 Aug 98	27.80	91.41	490	n.m.	0.025	0.98
MSI3	06 May 98	27.74	90.77	831	34.9	0.036	0.94
MC3	06 May 98	27.96	89.47	1083	34.9	0.050	0.97
MSI2	16 Aug 98	27.19	91.40	2270	n.m.	0.012	0.98

Abbreviations: Accum., accumulation; ASh, Atchafalaya Shelf; MSh, Mississippi Shelf; MC, Mississippi Canyon; MSI, Mississippi Slope; n.m., not measured.

were assumed to be similar to those from adjacent sites. A surface mixed layer of uniform excess ^{210}Pb activity was present in some cores (MSh1, MSh4, MC1; <10 cm thick). These samples were omitted from the sediment accumulation calculations under the assumption that downcore mixing of ^{210}Pb by biological or physical means influenced measured activity.

2.3.2. Elemental analysis

Total carbon (TC) and total nitrogen (TN) contents were measured by high temperature combustion on a Perkin Elmer 2400 Elemental Analyzer. Organic carbon (OC) content was similarly measured, but with vapor phase-acidification preceding combustion (Hedges and Stern, 1984). Inorganic carbon (IC) content was determined by difference (TC–OC). The average standard deviation of each measurement, determined by replicate analysis of the same sample, was ± 0.02 wt.%.

2.3.3. Stable carbon isotopes

Samples were acidified with 1 N HCl to remove inorganic carbon prior to carbon isotopic measurements. Stable carbon isotope composition of the sedimentary OM was determined by on-line combustion in a Fisons elemental analyzer interfaced to a VG Optima stable isotope ratio mass spectrometer. $^{13}\text{C}/^{12}\text{C}$ is expressed in ‰ relative to the PDB standard by the conventional δ notation. Analytical precision, determined by replicate analysis of the same sample, was ± 0.3 ‰.

2.3.4. BET surface area

Mineral surface area was determined using a Coulter SA3100 Surface Area Analyzer. Approximately 1 g of unground sediment was rinsed with deionized water and combusted for 12 h at 350 °C. Immediately prior to SA determination, the samples were outgassed at 250 °C for 1 h under vacuum. Surface area was then determined by a 5-point BET multilayer adsorption analysis (Brunauer et al., 1938). Analytical precision, determined from triplicate analysis of the same sample, was ± 0.1 m²/g.

2.3.5. CuO oxidation

CuO oxidation of samples was performed using a microwave digestion system described by Goñi and

Montgomery (2000). Approximately 400 mg of sediment was oxidized under alkaline (2 N NaOH) conditions with CuO at 151 °C for 1.5 h in N₂-pressurized teflon vessels. A recovery standard composed of ethylvanillin and *trans*-cinnamic acid was added immediately following oxidation. After acidification with concentrated HCl to pH 1, samples were extracted into ethyl acetate, blown to dryness with N₂, and dissolved in pyridine. The extract was stored frozen until gas chromatographic (GC) analysis. The oxidation products were derivatized with bis(trimethylsilyl) trifluoroacetamide (BSTFA)+1% trimethylchlorosilane (TMCS) and injected onto a HP6890 GC equipped with a 60 m DB1 column (J&W Scientific) using either on-column or splitless injection. Compound identification was verified by gas chromatography/mass spectrometry (GC/MS) on a Varian Saturn 2000 Ion Trap GC/MS.

2.3.6. Radiocarbon analysis

Radiocarbon analyses were performed at the National Ocean Sciences Accelerator Mass Spectrometry (NOSAMS) facility at Woods Hole Oceanographic Institution following established procedures (Vogel et al., 1987; McNichol et al., 1992). CO₂ gas, produced by the combustion of sedimentary OC, was converted to graphite via Fe/H₂ catalytic reduction. The graphite was pressed into AMS targets and analyzed on the AMS. Radiocarbon values are reported as Fraction modern (F_m), which is calculated according to Stuiver and Polach (1977): $F_m = (S - B) / (M - B)$, where S , B , and M are the $^{14}\text{C}/^{12}\text{C}$ ratios of sample, blank, and modern reference material, and the reported F_m is corrected for fractionation. Conventional radiocarbon ages ($t = -8033 \ln(F_m)$) and $\Delta^{14}\text{C}$ ($= (F_m e^{-\lambda(y-1950)} - 1) \times 1000$, where $\lambda = 1/8267$ year⁻¹ and y is the year of measurement; Stuiver and Polach, 1977) are also reported.

3. Results and discussion

3.1. Organic matter accumulation in a river-dominated margin

Despite its significance in the global carbon cycle, the content and composition of OM in marine

sediments, as well as the factors that control its distribution, remain poorly understood. Berner (1982) estimated a carbon deposition rate of 130 Mt/year in marine sediments, 80% of which was presumed to accumulate in deltaic and shelf sediments. Hedges and Keil (1995) revised this percentage upwards

(ca. 90%) to account for the greater OC content of non-deltaic shelf sediments than was assumed by Berner (1982). Other recent studies (e.g., de Haas et al., 2002) suggest that cross-shelf transport of OM to the slope is a significant process in the oceanic accumulation of OM. Although slope

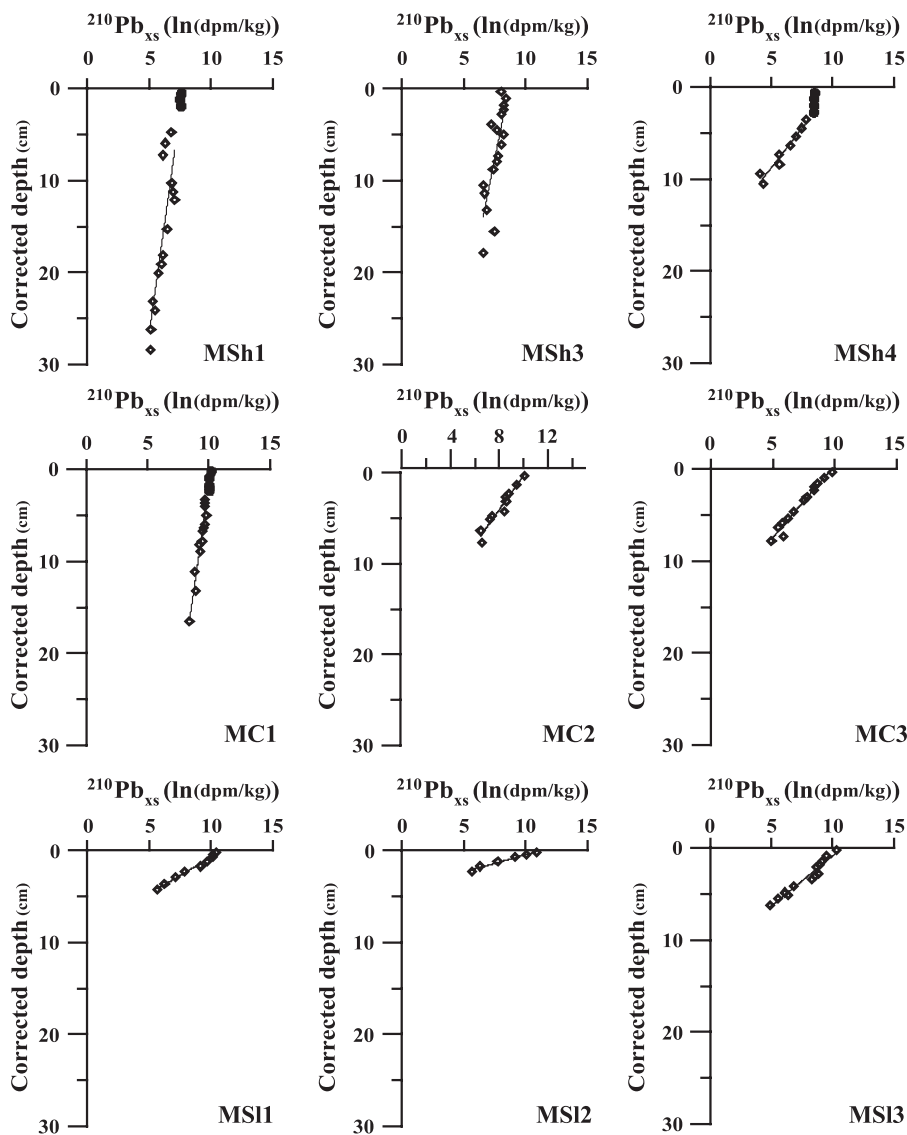


Fig. 2. Excess ^{210}Pb activity in Mississippi margin box cores. The natural log of total (\bullet) and excess (\diamond) ^{210}Pb ($^{210}\text{Pb}_{\text{xs}}$) activity, measured by alpha counting (see Methods), is plotted versus the corrected depth, which is the sampling depth corrected to 75% porosity (y -axis). The total activity is shown only in cores that indicated a surface mixed layer, the activity of which was not used in the sediment accumulation calculation. The linear relationship between $\ln(^{210}\text{Pb}_{\text{xs}})$ and sediment depth, which was used to calculate the accumulation rate, is indicated. The ^{210}Pb accumulation rates for the four Atchafalaya margin cores and one Mississippi shelf core (MSh2) have been previously published (Allison et al., 2000).

Table 2
Elemental, isotopic, and surface area composition of box core samples

Station	Depth (cm)	%OC salt-free	%TN salt-free	C/N	%CaCO ₃	δ ¹³ C (‰)	BET SA (m ² /g)	Δ ¹⁴ C (‰)	¹⁴ C age (ybp)	F _m	
ASh1	0–1	1.35	0.17	9.1 (1.1)	2.1	–22.5	38.0	–203.3	1780	0.80	
	2–3	1.37	0.17	9.4 (1.1)	2.2	–22.7					
	4–5	1.14	0.14	9.7 (1.4)	2.1	–22.5					
	6–7	1.19	0.15	9.5 (1.3)	2.1	–22.3					
	8–9	1.25	0.12	12.6 (2.2)	2.0	–22.8					
	10–11	1.36	0.15	10.9 (1.5)	1.8	–22.6					
	13–14	1.15	0.11	12.4 (2.3)	2.0	–22.5					
	15–16	1.28	0.09	16.2 (3.5)	n.m.	–22.5					
	19–20	1.20	0.15	9.5 (1.3)	3.1	–22.4					
	20–22	1.01	0.08	15.0 (3.8)	2.3	–22.8					
	24–26	1.06	0.12	10.2 (1.7)	1.6	–22.3					
	28–30	1.04	0.11	11.0 (2.0)	1.9	–22.5					
	<i>Synchron</i>	1.20 (0.12)	0.13 (0.03)	11.3 (2.3)	1.9 (0.7)	–22.5 (0.2)	38.0	–203.3	1780	0.80	
	ASh2	1–2	1.28	0.13	11.4 (1.7)	2.9	–22.6	44.4	–222.7	1970	0.78
4–5		1.17	0.12	11.1 (1.8)	n.m.	–22.6					
6–7		1.19	0.14	9.6 (1.3)	4.1	–22.6					
8–9		1.28	0.11	13.6 (2.5)	n.m.	–22.5					
11–12		1.19	0.17	8.4 (1.0)	1.6	–22.1					
13–14		1.18	0.16	8.6 (1.1)	1.6	–22.4					
15–16		1.14	0.11	11.7 (2.1)	n.m.	–22.9					
19–20		1.32	0.16	9.4 (1.2)	1.7	–22.2					
22–24		1.10	0.13	10.1 (1.6)	1.8	–22.1					
26–28		1.21	0.15	9.3 (1.2)	1.6	–22.2					
<i>Synchron</i>		1.21 (0.07)	0.14 (0.02)	10.3 (1.6)	1.5 (1.3)	–22.4 (0.2)	44.4	–222.7	1970	0.78	
ASh3		0–1	0.67	0.10	7.9 (1.6)	3.7	–21.2	19.8	–278.3	2570	0.73
		2–3	0.71	0.06	13.0 (4.1)	3.5	–21.1				
		4–5	0.69	0.04	20.9	3.8	–22.1				
	6–7	0.66	0.11	7.1 (1.3)	4.1	–21.3					
	8–9	0.64	0.06	13.0 (4.5)	3.9	–21.5					
	10–11	0.65	0.08	9.5 (2.4)	3.5	–21.6					
	13–14	0.56	0.09	7.0 (1.5)	3.7	–22.6					
	15–16	0.53	0.07	9.3 (2.8)	3.8	–22.7					
	19–20	0.50	0.05	11.1 (4.2)	3.5	–22.6					
	<i>Synchron</i>	0.63 (0.07)	0.07 (0.02)	11.0 (4.4)	3.7 (0.2)	–21.9 (0.7)	19.8	–278.3	2570	0.73	
	ASh4	0–1	0.55	0.08	8.0 (2.0)	3.6	–21.3	14.5	–252.9	2290	0.75
		2–3	0.62	0.10	7.1 (1.4)	2.8	–20.8				
		4–5	0.59	0.06	11.0 (3.5)	2.6	–21.5				
		6–7	n.m.	n.m.	n.m.	n.m.	–21.4				
8–9		0.55	0.09	7.1 (1.6)	2.9	–21.4					
11–12		0.53	0.06	10.2 (3.4)	2.7	–21.2					
13–14		0.48	0.07	7.9 (2.3)	3.3	–21.5					
<i>Synchron</i>		0.56 (0.05)	0.08 (0.02)	8.5 (1.6)	3.0 (0.4)	–21.3 (0.2)	14.5	–252.9	2290	0.75	
MSh1		0–1	0.60	0.09	8.2 (1.9)	4.1	–22.3	21.9	–323.0	3080	0.68
		2–3	0.56	0.07	9.4 (2.7)	4.1	–22.2				
		4–5	0.29	0.05	6.3 (2.3)	4.9	–22.6				
		6–7	0.65	0.07	10.5 (2.9)	4.3	–22.6				
		8–9	0.70	0.07	12.4 (3.7)	3.9	–22.7				
		10–11	0.87	0.05	21.0 (8.7)	8.0	–22.7				
	12–13	0.51	0.05	11.7 (4.6)	5.3	–22.7					
	14–15	0.65	0.10	7.7 (1.6)	5.0	–23.4					
	16–17	0.57	0.05	12.6 (4.8)	3.2	–23.0					

(continued on next page)

Table 2 (continued)

Station	Depth (cm)	%OC salt-free	%TN salt-free	C/N	%CaCO ₃	$\delta^{13}\text{C}$ (‰)	BET SA (m ² /g)	$\Delta^{14}\text{C}$ (‰)	¹⁴ C age (ybp)	F _m
MSh2	18–19	0.53	0.07	8.9 (2.6)	5.3	–22.9				
	20–22	0.40	0.12	3.7 (0.6)	3.9	–23.2				
	24–26	0.40	0.10	4.6 (0.9)	3.2	–23.1				
	<i>Synchron</i>	0.56 (0.15)	0.07 (0.02)	9.7 (4.6)	4.6 (1.3)	–22.8 (0.4)	21.9	–323.0	3080	0.68
	0–1	1.06	0.14	8.6 (1.2)	3.3	–21.5	21.8	n.m.	n.m.	n.m.
	2–3	0.72	0.09	9.1 (2.0)	3.5	–21.6				
	4–5	0.70	0.10	8.3 (1.7)	3.7	–22.0				
MSh3	6–7	0.76	0.07	12.3 (3.5)	n.m.	–24.4				
	<i>Synchron</i>	0.81 (0.17)	0.11 (0.03)	9.6 (1.8)	3.5 (0.2)	–22.4 (1.4)	21.8			
	0–1	1.08	0.15	8.5 (1.2)	2.9	–21.5	34.4	–226.5	2010	0.78
	2–3	1.03	0.13	9.5 (1.5)	3.1	–21.3				
	4–5	0.99	0.13	9.1 (1.4)	3.1	–21.8				
	6–7	1.00	0.12	9.7 (1.6)	3.1	–22.2				
	8–9	0.92	0.13	8.4 (1.3)	2.9	–21.8				
	11–12	0.79	0.10	9.2 (1.9)	3.2	–22.5				
	13–14	0.84	0.12	8.0 (1.3)	3.4	–21.8				
	15–16	0.80	0.08	11.7 (3.0)	3.8	–21.9				
	17–18	0.82	0.09	10.1 (2.2)	3.4	–21.8				
	19–20	0.80	0.11	8.2 (1.5)	3.4	–22.0				
	20–22	0.65	0.09	8.3 (1.8)	3.6	–22.2				
	24–26	0.64	0.07	10.0 (2.7)	3.2	–23.3				
MSh4	<i>Synchron</i>	0.86 (0.14)	0.11 (0.02)	9.2 (1.1)	3.3 (0.3)	–21.9 (0.3)	34.4	–226.5	2010	0.78
	0–1	0.68	0.09	8.7 (1.9)	4.8	–22.0	24.7	–452.2	4780	0.55
	2–3	0.65	0.08	9.6 (2.5)	5.3	–22.6				
	4–5	0.62	0.07	10.0 (2.8)	4.5	–23.2				
	6–7	0.63	0.07	11.1 (3.4)	4.0	–23.2				
MC1	<i>Synchron</i>	0.64 (0.03)	0.07 (0.01)	9.8 (1.0)	4.7 (0.5)	–22.9 (0.4)	24.7	–452.2	4780	0.55
	0–1	1.50	0.17	10.0 (1.2)	3.0	–21.5	58.6	–228.6	2030	0.78
	2–3	1.41	0.18	9.2 (1.0)	3.7	–21.5				
	4–5	1.40	0.17	9.4 (1.1)	3.9	–21.4				
	6–7	1.36	0.17	9.3 (1.1)	3.7	–21.4				
	8–9	1.39	0.17	9.7 (1.2)	3.1	–21.2				
	10–11	1.27	0.17	8.9 (1.1)	3.6	–21.2				
	12–13	1.28	0.16	9.4 (1.2)	3.4	–21.3				
	14–15	1.28	0.16	9.3 (1.2)	3.6	–21.1				
	16–17	1.23	0.15	9.2 (1.2)	3.4	–21.4				
	18–19	1.18	0.15	9.0 (1.2)	3.3	–21.3				
	20–22	1.13	0.14	9.2 (1.3)	3.6	–21.6				
	24–26	1.07	0.13	9.5 (1.5)	4.0	–21.5				
	MC2	<i>Synchron</i>	1.29 (0.13)	0.16 (0.01)	9.3 (0.3)	3.5 (0.3)	–21.4 (0.1)	58.6	–228.6	2030
0–1		1.37	0.15	10.4 (1.4)	10.3	–21.8	55.0	–262.6	2400	0.74
2–3		1.16	0.15	9.1 (1.2)	11.4	–21.1				
MS11	<i>Synchron</i>	1.22 (0.13)	0.15 (0.01)	9.8 (0.9)	11.2 (0.8)	–21.3 (0.4)	55.0	–262.6	2400	0.74
	0–1	1.27	0.20	7.3 (0.7)	13.0	–21.3	56.0	–278.4	2570	0.73
MS13	<i>Synchron</i>	1.27	0.20	7.3	13.0	–21.3	56.0	–278.4	2570	0.73
	0–1	1.38	0.14	11.9 (1.8)	12.8	–20.2	52.7	–309.1	2920	0.70
MC3	2–3	1.12	0.14	9.2 (1.3)	12.3	–21.0				
	<i>Synchron</i>	1.25 (0.19)	0.14 (0.00)	10.6 (1.9)	12.6 (0.3)	–20.6 (0.5)	52.7	–309.1	2920	0.70
	0–1	1.59	0.15	12.2 (1.6)	6.2	–20.9	60.3	–286.0	2650	0.72
	1–2	1.41	0.15	10.7 (1.4)	8.0	–20.7				
	3–4	1.20	0.14	10.0 (1.4)	9.6	–20.7				
MS12	<i>Synchron</i>	1.40 (0.19)	0.15 (0.01)	11.0 (1.1)	7.9 (1.7)	–20.8 (0.1)	60.3	–286.0	2650	0.72
	0–1	1.14	0.13	10.2 (1.6)	23.8	–22.1	43.3	–359.5	3530	0.64
	<i>Synchron</i>	1.14	0.13	10.2	23.8	–22.1	43.3	–359.5	3530	0.64

sediments generally contain greater OC contents than shelf sediments (Premuzic et al., 1982), no consensus exists on the most important sites of OM burial in the modern ocean, and the processes that control this accumulation remain elusive. The accumulation of OM in the present study area is quantified in order to examine the relative importance of the shelf versus the slope in the potential sequestration of carbon in a river-dominated margin.

Sediment accumulation rates were determined from ^{210}Pb profiles of sediments from 14 sampling locations in the study area (Table 1; Fig. 2). Calculated sediment accumulation rates range from 0.012 to 0.68 cm/year (Table 1) and show an inverse logarithmic relationship with water depth ($r^2=0.56$). Values are highest along the inner shelf (>0.5 cm/year), with slower rates (0.2–0.3 cm/year) on the outer shelf. Sedimentation rates on the slope range from a high of 0.31 cm/year at 365 m water depth to 0.012 cm/year in the most distal basin (2270 m water depth). Such a wide range in sediment accumulation rates across the margin makes compositional comparisons among surficial sediments difficult due to the different sedimentation history of particles accumulating at each site. For example, while the 0–1 cm interval of sediment in the inner shelf sites represents ca. 1 year of sedimentation, the same interval at the most distal region represents nearly 100 years of deposition. Thus, to appropriately compare OM content and composition between sites, elemental, isotopic, and lignin biomarker signatures of several sediment horizons that span similar time intervals were averaged (Tables 2–4). These synchronous sediment intervals (synchons), ranging from 0–1 cm at the most distal sampling location to 0–26 cm at the inner shelf locations, represent ca. 80 years of sedimentation.

The OC, TN, and lignin accumulation rates from each station (Table 5) were calculated as the product of sediment accumulation rates (Table 1) and chemical composition of the synchons (Tables 2

and 3). The annual fluxes of sediment, OC, TN, and lignin to the study area were then determined as the product of the average accumulation rates at stations located on the inner shelf (0–10 m water depth), outer shelf (10–200 m water depth), and slope (200–2000 m water depth) and the areal extent of each region (Table 5). The area of each region was defined based on bathymetry between the longitudes 89.4°W and 92.5°W (Fig. 1). The major assumption in these calculations is that the average compositions determined from the sites sampled are representative of the overall areas.

The inner shelf region accounts for 31% of the sediment accumulation for the study region, though it occupies only 9% of the accumulation area (Fig. 3a). Nearly half of the sediment accumulation (45%) occurs on the outer shelf, with the remaining 24% of sediment accumulating in the slope region. OC and TN accumulation show a similar spatial pattern (Fig. 3b,c), with approximately 35% of the OC and TN accumulating on the inner shelf. Annual OM accumulation on the outer shelf is less than the inner shelf, despite the greater areal extent of the outer versus the inner shelf. The slope, which occupies the greatest area, accounts for a similar proportion of the OC and TN accumulation (33%) as the inner and outer shelf areas. This proportion is higher than expected, given the low sediment accumulation rates measured for slope stations in this study, and previous estimates of OM accumulation in slope regions. For example, Berner (1989) estimated that the slope accounted for 6% of global OM burial, while Hedges and Keil (1995) revised that estimate to 4%. The results from the present study indicate that slope sediments, especially those located offshore of river-dominated margins, may play a greater role in OM accumulation than previously considered. This result is consistent with the suggestion of de Haas et al. (2002) that cross-shelf transport and accumulation of OM in slope sediments represents a quantitatively important process in the oceanic OM cycle. These results, while not representative of the entire global oceanic

Notes to Table 2:

The standard deviation for C/N, reported in italics, was calculated on the basis of propagation of error (Taylor, 1982). The composition of the synchron is the average of the reported intervals for each core. The range of observed values, calculated as one standard deviation, is presented in parentheses. Note that only surface values are reported for SA and radiocarbon.

Table 3
Molecular composition of sediment samples

Station	Depth (cm)	S (mg/100 mg OC)	V (mg/100 mg OC)	C (mg/100 mg OC)	A (mg/100 mg OC)	B (mg/100 mg OC)	P (mg/100 mg OC)
ASh1	0–1	0.97 (0.16)	0.89 (0.05)	0.21 (0.03)	2.08 (0.24)	0.33 (0.11)	0.39 (0.06)
	2–3	1.10	1.10	0.27	2.47	0.32	0.42
	6–7	0.81	0.73	0.17	1.71	0.33	0.30
	13–14	0.80	0.72	0.16	1.68	0.34	0.33
	20–22	0.98	0.94	0.20	2.12	0.29	0.31
	28–30	0.91	0.87	0.17	1.95	0.28	0.29
	<i>Synchron</i>	0.93 (0.11)	0.87 (0.14)	0.20 (0.04)	2.00 (0.29)	0.32 (0.02)	0.34 (0.05)
ASh2	1–2	0.73 (0.07)	0.69 (0.05)	0.17 (0.05)	1.59 (0.17)	0.23 (0.06)	0.31 (0.03)
	4–5	1.01	1.01	0.27	2.29	0.31	0.41
	6–7	0.76	0.70	0.17	1.62	0.32	0.29
	13–14	0.73	0.67	0.17	1.57	0.29	0.26
	19–20	1.12	1.08	0.28	2.48	0.32	0.37
	26–28	0.69	0.62	0.13	1.44	0.29	0.26
	<i>Synchron</i>	0.84 (0.18)	0.79 (0.20)	0.20 (0.06)	1.83 (0.44)	0.29 (0.02)	0.32 (0.06)
ASh3	0–1	0.45 (0.09)	0.40 (0.05)	0.084 (0.016)	0.93 (0.16)	0.27 (0.10)	0.31 (0.07)
	2–3	0.49	0.48	0.11	1.08	0.29	0.30
	6–7	0.72 (0.22)	0.54 (0.05)	0.10 (0.02)	1.37 (0.29)	0.31 (0.04)	0.34 (0.08)
	13–14	0.62 (0.02)	0.58 (0.07)	0.11 (0.01)	1.31 (0.10)	0.28 (0.05)	0.22 (0.02)
	19–20	0.51	0.48	0.081	1.07	0.28	0.19
	<i>Synchron</i>	0.56 (0.11)	0.49 (0.07)	0.10 (0.01)	1.15 (0.18)	0.29 (0.02)	0.27 (0.06)
ASh4	0–1	0.39 (0.05)	0.42 (0.04)	0.093 (0.025)	0.90 (0.12)	0.19 (0.05)	0.32 (0.09)
	2–3	0.49	0.49	0.11	1.10	0.28	0.30
	6–7	0.58	0.52	0.090	1.19	0.31	0.26
	8–9	0.65	0.58	0.11	1.33	0.36	0.29
	13–14	0.84	0.77	0.12	1.73	0.29	0.29
	<i>Synchron</i>	0.59 (0.17)	0.55 (0.13)	0.10 (0.01)	1.25 (0.31)	0.29 (0.06)	0.29 (0.02)
MSh1	0–1	0.80	0.95	0.18	1.94	0.61	0.53
	2–3	1.07	1.08	0.20	2.35	0.45	0.59
	6–7	1.42	1.14	0.30	2.87	0.31	0.34
	12–13	1.26	1.37	0.15	2.77	0.38	0.48
	16–17	1.39	1.15	0.25	2.78	0.18	0.32
	24–26	1.17	1.02	0.19	2.38	0.16	0.32
	<i>Synchron</i>	1.18 (0.23)	1.12 (0.14)	0.21 (0.06)	2.51 (0.36)	0.35 (0.17)	0.43 (0.12)
MSh2	0–1	0.90 (0.06)	0.72 (0.02)	0.19 (0.03)	1.82 (0.10)	0.27 (0.19)	0.35 (0.04)
	6–7	0.92	0.82	0.10	1.85	0.26	0.25
	<i>Synchron</i>	0.91 (0.01)	0.77 (0.07)	1.83 (0.02)	1.83 (0.02)	0.26 (0.01)	0.30 (0.07)
MSh3	0–1	0.49 (0.01)	0.40 (0.02)	0.11 (0.02)	1.00 (0.04)	0.26 (0.18)	0.50 (0.25)
	2–3	0.47	0.44	0.12	1.03	0.24	0.22
	6–7	0.75	0.60	0.19	1.53	0.17	0.34
	11–12	0.69	0.52	0.18	1.39	0.17	0.23
	17–18	0.72 (0.00)	0.64 (0.00)	0.17 (0.00)	1.52 (0.01)	0.15 (0.00)	0.29 (0.01)
	24–26	0.71	0.62	0.17	1.50	0.14	0.28
<i>Synchron</i>	0.64 (0.12)	0.53 (0.10)	0.16 (0.03)	1.33 (0.25)	0.19 (0.05)	0.31 (0.10)	
MSh4	0–1	0.67	0.68	0.058	1.41	0.42	0.30
	6–7	0.61	0.57	0.11	1.29	0.18	0.17
	<i>Synchron</i>	0.64 (0.04)	0.62 (0.08)	0.081 (0.033)	1.35 (0.09)	0.30 (0.17)	0.24 (0.09)
MC1	0–1	0.29 (0.06)	0.25 (0.04)	0.067 (0.031)	0.60 (0.14)	0.27 (0.05)	0.17 (0.05)
	2–3	0.20	0.23	0.062	0.49	0.26	0.16
	6–7	0.27	0.21	0.067	0.55	0.22	0.14
	12–13	0.18	0.21	0.040	0.43	0.22	0.22
	16–17	0.17	0.20	0.034	0.41	0.26	0.20

Table 3 (continued)

Station	Depth (cm)	S (mg/100 mg OC)	V (mg/100 mg OC)	C (mg/100 mg OC)	A (mg/100 mg OC)	B (mg/100 mg OC)	P (mg/100 mg OC)
MC2	24–26	0.33	0.30	0.076	0.71	0.12	0.16
	<i>Synchron</i>	0.24 (0.06)	0.23 (0.04)	0.058 (0.017)	0.53 (0.11)	0.22 (0.06)	0.17 (0.03)
	0–1	0.18	0.13	0.025	0.33	0.25	0.12
	2–3	0.099	0.10	0.054	0.26	0.27	0.11
MS11	<i>Synchron</i>	0.14 (0.05)	0.11 (0.02)	0.040 (0.02)	0.29 (0.05)	0.26 (0.02)	0.12 (0.01)
	0–1	0.13 (0.01)	0.12 (0.01)	0.026 (0.01)	0.28 (0.02)	0.20 (0.01)	0.12 (0.022)
MS13	<i>Synchron</i>	0.13	0.12	0.026	0.28	0.20	0.12
	0–1	0.23	0.079	0.019	0.33	0.14	0.087
MC3	2–3	0.29	0.37	0.032	0.70	0.21	0.21
	<i>Synchron</i>	0.26 (0.05)	0.23 (0.21)	0.025 (0.010)	0.51 (0.26)	0.17 (0.05)	0.15 (0.09)
	0–1	0.090 (0.13)	0.069 (0.017)	0.017 (0.015)	0.18 (0.04)	0.092 (0.017)	0.057 (0.022)
	3–4	0.045	0.065	0.019	0.13	0.17	0.053
MS12	<i>Synchron</i>	0.068 (0.032)	0.067 (0.003)	0.018 (0.002)	0.15 (0.03)	0.13 (0.05)	0.055 (0.002)
	0–1	0.15 (0.00)	0.13 (0.01)	0.026 (0.01)	0.30 (0.02)	0.20 (0.02)	0.11 (0.01)
	<i>Synchron</i>	0.15	0.13	0.026	0.30	0.20	0.11

One standard deviation about the mean is reported in parentheses for samples that were processed in replicate. The synchron composition is the average of the reported intervals for each core, and the range of values is calculated as one standard deviation, presented in parentheses. Abbreviations: S, syringyl phenols; V, vanillyl phenols; C, cinnamyl phenols; A, B, benzoic acids; P, *p*-hydroxybenzenes.

margin, suggest that OM burial in slope regions warrants further attention.

In contrast to bulk OM, lignin accumulation is concentrated (61%) on the inner shelf (Fig. 3d). The delivery of terrigenous OM to the inner shelf via the Atchafalaya mud stream is partly responsible for the observed trend. The overwhelming accumulation of lignin-bearing OM on the inner shelf is somewhat surprising, however, given that only 31% of particle deposition occurs in this region, and that lignin content (mg/gdw) varies significantly with sediment accumulation rates ($r^2=0.69$). Such disproportionate accumulation may be due to the heterogeneous chemical character of the lignin-bearing OM. Coarse plant fragments, such as woody debris, contain higher levels of lignin than non-woody and soil-derived OM (e.g., Hedges et al., 1986; Goñi and Thomas, 2000). The deposition of coarse debris close to shore has been observed in the Atchafalaya Delta (Gordon and Goñi, 2003) and in the lower reaches of the Mississippi mainstem (Bianchi et al., 2002). Differential deposition of lignin-rich components would result in elevated lignin accumulation rates on the inner shelf. Despite its low accumulation seaward of the shelf break (2%), lignin remains a measurable component of the sedimentary OM deposited in deeper regions of the margin.

The disproportionately large accumulation of OM on the inner shelf highlights the importance of shelves as oceanographic OM depocenters, especially in a region of rising sea level such as the northern Gulf of Mexico (e.g., Penland and Ramsey, 1990). That the majority of the accumulation for all organic constituents in the present study area occurs in shallow water (<10 m), despite its limited areal extent (9% of the study region) suggests a significant role of the inner shelf in OM sequestration. One caveat, however, is that the aforementioned rates represent the material that is accumulating on the seabed over the past 80 years, rather than estimates of longer-term burial. The inner Atchafalaya shelf is a site of intense sediment reworking (e.g., Allison et al., 2000) and is under the direct influence of the Atchafalaya mud stream, which may be a site of elevated OM remineralization. Aller (1998) reported high OM turnover rates in the Amazon “mobile mud belt” due to the resuspension of OM and its exposure to oscillating redox conditions. The Atchafalaya mud stream, which may be analogous to the Amazon mobile mud belt due to its comparable layer of unconsolidated mud (Velasco, 2003), is a region in which much of the OM that initially accumulates might eventually be remineralized. The extensive summer hypoxia in the northern Gulf of Mexico (e.g., Rabalais et al., 1999) and the

Table 4
Lignin compositional parameters

Station	Depth (cm)	S/V	C/V	3,5 Bd/V	Sd/SI	Vd/VI
ASh1	0–1	1.09 (0.19)	0.23 (0.04)	0.15 (0.11)	0.42 (0.15)	0.43 (0.05)
	2–3	1.01	0.24	0.086	0.40	0.46
	6–7	1.12	0.24	0.27	0.40	0.40
	13–14	1.12	0.22	0.28	0.41	0.39
	20–22	1.04	0.22	0.19	0.37	0.37
	28–30	1.05	0.20	0.22	0.37	0.38
	<i>Synchron</i>	1.07 (0.05)	0.22 (0.02)	0.20 (0.07)	0.40 (0.02)	0.40 (0.03)
ASh2	1–2	1.07 (0.13)	0.25 (0.07)	0.14 (0.10)	0.39 (0.05)	0.44 (0.10)
	4–5	1.01	0.27	0.10	0.43	0.47
	6–7	1.09	0.24	0.28	0.40	0.44
	13–14	1.08	0.25	0.24	0.46	0.39
	19–20	1.04	0.26	0.19	0.39	0.37
	26–28	1.10	0.22	0.30	0.39	0.41
	<i>Synchron</i>	1.06 (0.04)	0.25 (0.02)	0.21 (0.08)	0.41 (0.03)	0.42 (0.03)
ASh3	0–1	1.12 (0.27)	0.22 (0.05)	0.31 (0.22)	0.62 (0.23)	0.53 (0.15)
	2–3	1.03	0.24	0.13	0.40	0.44
	6–7	1.33 (0.42)	0.19 (0.04)	0.35 (0.04)	0.46 (0.22)	0.44 (0.05)
	13–14	1.07 (0.13)	0.18 (0.02)	0.23 (0.05)	0.51 (0.06)	0.44 (0.07)
	19–20	1.06	0.17	0.24	0.40	0.38
	<i>Synchron</i>	1.13 (0.13)	0.20 (0.03)	0.24 (0.08)	0.47 (0.09)	0.45 (0.05)
ASh4	0–1	0.94 (0.15)	0.22 (0.06)	0.090 (0.05)	0.72 (0.14)	0.59 (0.12)
	2–3	1.00	0.23	0.13	0.41	0.43
	6–7	1.11	0.17	0.31	0.48	0.36
	8–9	1.13	0.19	0.30	0.57	0.42
	13–14	1.10	0.15	0.21	0.40	0.38
	<i>Synchron</i>	1.06 (0.08)	0.19 (0.03)	0.21 (0.10)	0.51 (0.13)	0.43 (0.09)
MSh1	0–1	0.84	0.19	0.35	0.63	0.45
	2–3	0.99	0.18	0.049	0.36	0.34
	6–7	1.25	0.27	0.18	0.32	0.38
	12–13	0.92	0.11	0.082	0.66	0.62
	16–17	1.21	0.22	0.053	0.27	0.32
	24–26	1.14	0.18	0.043	0.28	0.31
	<i>Synchron</i>	1.06 (0.17)	0.19 (0.05)	0.13 (0.12)	0.42 (0.18)	0.40 (0.12)
MSh2	0–1	1.25 (0.08)	0.27 (0.04)	0.17 (0.24)	0.36 (0.05)	0.39 (0.05)
	6–7	1.12	0.12	0.17	0.33	0.33
	<i>Synchron</i>	1.19 (0.10)	0.20 (0.10)	0.17 (0.00)	0.35 (0.02)	0.36 (0.04)
MSh3	0–1	1.23 (0.05)	0.28 (0.05)	0.31 (0.35)	0.55 (0.10)	0.51 (0.05)
	2–3	1.08	0.28	0.12	0.40	0.41
	6–7	1.26	0.32	0.081	0.48	0.55
	11–12	1.32	0.34	0.053	0.45	0.53
	17–18	1.13 (0.01)	0.26 (0.00)	0.073 (0.001)	0.45 (0.02)	0.51 (0.01)
	24–26	1.15	0.27	0.072	0.41	0.47
	<i>Synchron</i>	1.19 (0.09)	0.29 (0.03)	0.12 (0.10)	0.46 (0.05)	0.50 (0.05)
MSh4	0–1	1.00	0.085	0.30	0.57	0.48
	6–7	1.08	0.18	0.14	0.41	0.47
	<i>Synchron</i>	1.04 (0.06)	0.13 (0.07)	0.22 (0.11)	0.49 (0.11)	0.47 (0.00)
MC1	0–1	1.15 (0.32)	0.27 (0.13)	0.61 (0.12)	0.57 (0.28)	0.59 (0.08)
	2–3	0.87	0.27	0.27	0.52	0.59
	6–7	1.30	0.32	0.63	0.78	0.83
	12–13	0.85	0.19	0.28	0.65	0.70
	16–17	0.86	0.17	0.33	0.96	0.85
	24–26	1.08	0.25	0.098	0.54	0.61
	<i>Synchron</i>	1.02 (0.19)	0.24 (0.06)	0.37 (0.21)	0.65 (0.14)	0.69 (0.12)

Table 4 (continued)

Station	Depth (cm)	S/V	C/V	3,5 Bd/V	Sd/SI	Vd/VI
MC2	0–1	1.40	0.20	0.81	1.86	0.65
	2–3	0.96	0.53	0.48	0.67	0.94
	<i>Synchron</i>	1.18 (0.31)	0.36 (0.23)	0.64 (0.23)	1.27 (0.84)	0.80 (0.21)
MS11	0–1	1.13 (0.10)	0.22 (0.08)	0.68 (0.11)	1.85 (0.66)	0.57 (0.13)
	<i>Synchron</i>	1.13	0.22	0.68	1.85	0.57
MS13	0–1	2.91	0.23	0.13	0.25	0.56
	2–3	0.79	0.087	0.14	0.59	0.58
	<i>Synchron</i>	1.85 (1.50)	0.16 (0.10)	0.14 (0.01)	0.42 (0.24)	0.57 (0.01)
MC3	0–1	1.31 (0.38)	0.24 (0.23)	0.26 (0.20)	1.31 (3.71)	0.75 (0.28)
	3–4	0.70	0.30	0.44	0.61	0.82
	<i>Synchron</i>	1.00 (0.43)	0.27 (0.04)	0.35 (0.13)	0.96 (0.49)	0.79 (0.05)
MS12	0–1	1.17 (0.06)	0.21 (0.08)	0.71 (0.04)	2.24 (0.13)	0.51 (0.10)
	<i>Synchron</i>	1.17	0.21	0.71	2.24	0.51

One standard deviation about the mean is reported for samples that were processed in replicate, calculated by propagation of error. The “synchron” composition is the average of the reported intervals for each core, and the range of values is calculated as one standard deviation, presented in parentheses.

Abbreviations: S, syringyl phenols; V, vanillyl phenols; C, cinnamyl phenols; 3,5-Bd, 3,5-dihydroxybenzoic acid; Sd, syringic acid; SI, syringaldehyde; Vd, vanillic acid; VI, vanillin.

bacterial productivity observed in the Atchafalaya plume (Pakulski et al., 2000) are indicative of such a scenario. Regardless of the ultimate fate of this OM, either through burial, desorption, or remineralization,

the inner shelf appears to play a disproportionate role in the biogeochemistry of the coastal ocean. Greater sampling coverage of inner shelves is needed to evaluate the role of these regions in the global

Table 5

Sediment, OC, TN, and lignin accumulation rates for box core locations of the study area

Station	Interval (cm)	Sediment (g/cm ² /year)	OC (g/m ² /year)	TN (g/m ² /year)	Lignin (mg/m ² /year)
<i>Inner shelf (8.8 × 10⁹ m²)</i>					
ASh1	0–30	0.45	54.0 (5.6)	5.8 (1.3)	1070 (260)
ASh2	0–28	0.37	44.6 (2.5)	5.1 (0.8)	830 (230)
<i>Outer shelf (35 × 10⁹ m²)</i>					
ASh3	0–20	0.18	11.3 (1.3)	1.3 (0.4)	130 (30)
ASh4	0–14	0.12	6.7 (0.6)	0.9 (0.2)	83 (15)
MSh1	0–26	0.28	15.7 (4.3)	2.0 (0.6)	380 (80)
MSh2	0–7	0.061	4.9 (1.0)	0.7 (0.2)	100 (20)
MSh3	0–26	0.22	19.0 (3.1)	2.4 (0.5)	260 (50)
MSh4	0–7	0.037	2.4 (0.1)	0.3 (0.0)	32 (4)
<i>Slope (52 × 10⁹ m²)</i>					
MC1	0–26	0.21	28.8 (1.6)	3.6 (0.1)	150 (30)
MC2	0–3	0.041	5.0 (0.5)	0.6 (0.0)	15 (4)
MS11	0–1	0.017	2.2 (n.a.)	0.3 (n.a.)	6.0 (n.a.)
MS13	0–3	0.024	3.0 (0.4)	0.3 (0.0)	13 (9)
MC3	0–4	0.033	4.6 (0.6)	0.5 (0.0)	7.4 (3.3)
MS12	0–1	0.008	0.91 (n.a.)	0.1 (n.a.)	2.9 (n.a.)

Sediment accumulation rates are based on ²¹⁰Pb measurements. OC, TN, and lignin accumulation rates were calculated as the product of the sediment accumulation rate and the composition of the synchronous sediment interval (see text), the depth of which is tabulated (“Interval”). The range of OC, TN, and lignin accumulation rates, calculated as one standard deviation about the depth-averaged sediment intervals, is presented in parentheses. The areal extent of each region of the study area (inner shelf, outer shelf, slope) is parenthetically reported in italics. n.a., not applicable.

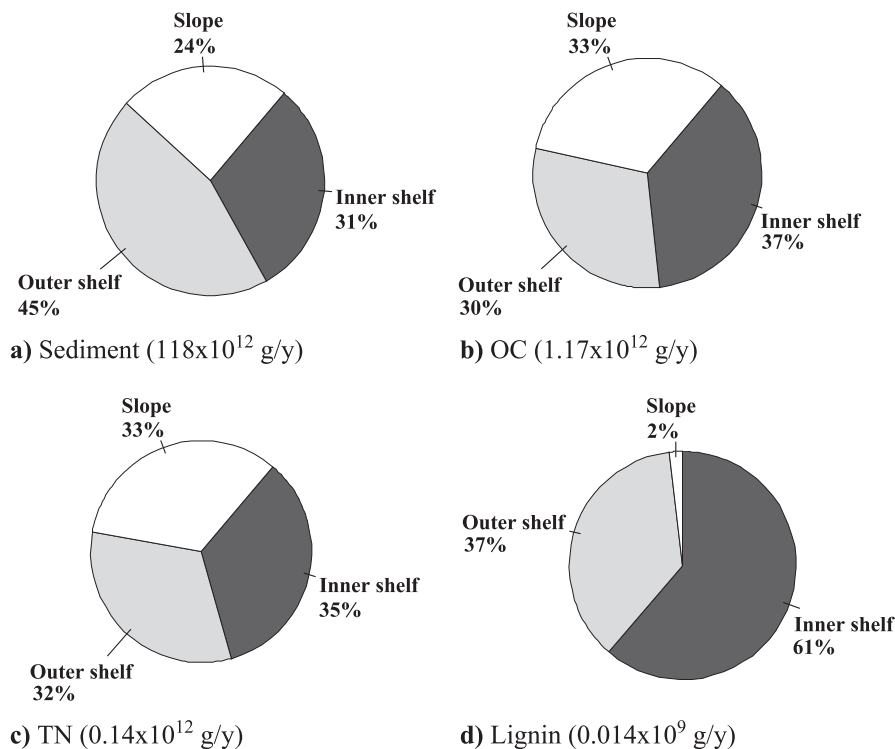


Fig. 3. Relative accumulation of (a) sediment, (b) OC, (c) TN, and (d) lignin from depositional regions of the study area. The inner shelf (<10 m water depth) is represented in black, the outer shelf (10–200 m water depth) is represented in gray, and the slope (>200 m water depth) is indicated in white. Relative accumulation rates are represented as percentages of accumulation (g/year).

remineralsation and burial of OM, particularly OM derived from land.

3.2. Compositional characteristics of sedimentary organic matter

The sediment dispersal patterns of the northern Gulf of Mexico exert an important control on both the accumulation and the composition of OM deposited on the Louisiana shelf (Gordon et al., 2001; Gordon and Goñi, 2003), and are likely responsible for observed trends in the study area. For example, organic carbon (OC) content along the shelf is higher at the inner shelf stations (ca. 1.3%) than the outer shelf stations (0.6–1.1%; Fig. 4) due to the dispersal of sediment parallel to the coastline within the 10 m isobath. OC content is higher at the slope stations (1.1 to 1.6%) relative to those inshore, with the highest value observed at the base of the Mississippi Canyon (1083 m water depth).

Overall, the relationship between %TN and %OC (Fig. 5) reveals a TN intercept that is within the TN analytical error (0.02 wt.%), consistent with the idea that most of the nitrogen measured in the shelf and slope sediments is associated with organic matter (Gordon et al., 2001). If we assume that most nitrogen present is organic nitrogen, the C/N ratios for synchrons throughout the study area range between 7.3 and 11.3 (Table 2; Fig. 4). The inner shelf sediments showed a higher average C/N (10.8) than the outer shelf (9.4) and slope sediments (9.7). In general, the observed C/N ratios are indicative of a mixture of marine phytoplankton (C/N~6.7; Redfield et al., 1963) and terrigenous sources, which contain lower levels of nitrogen than marine OM sources. The observed linear relationship between OC and TN (Fig. 5) and the similarity in C/N between the outer shelf and slope would require that the relative proportion of these two sources remain constant over a large range of water depths (14–2270 m). A more

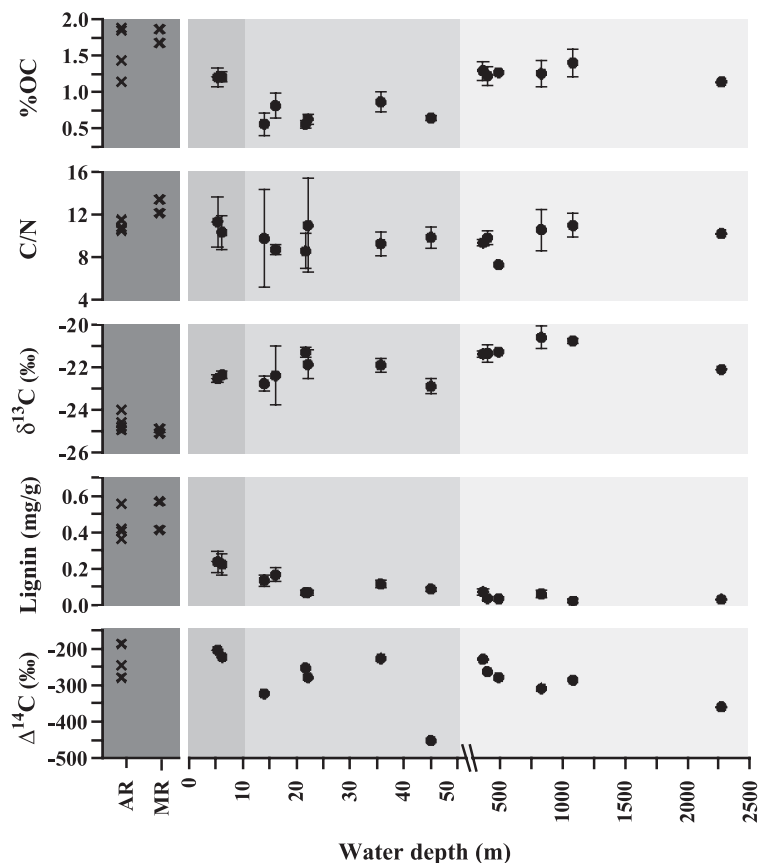


Fig. 4. Chemical composition of river suspended sediments, inner shelf, outer shelf, and slope sediments. %OC, C/N, $\delta^{13}\text{C}$ (‰), and lignin content (mg/g sed) of synchronous sediments, and $\Delta^{14}\text{C}$ (‰) of surface sediments, deposited in the inner shelf (<10 m water depth), outer shelf (10–200 m water depth), and slope (>200 m water depth) regions of the study area, indicated by gray shading. Water depth is indicated on the x-axis. AR, Atchafalaya River suspended sediments (SS); MR, Mississippi River SS. River SS data from Gordon and Goñi (2003).

likely scenario is that a significant portion of the sedimentary OM deposited in the outer shelf and slope is derived from a similar source. Soil-derived OM from the Mississippi drainage basin exhibits a C/N ratio between 10 and 13 (Tiessen et al., 1984; Parton et al., 1987); its delivery throughout the study area may explain the observed trend in elemental ratios.

The average stable carbon isotope composition ($\delta^{13}\text{C}_{\text{OC}}$) of shelf sediments is more depleted than the average value measured in deeper regions (Fig. 4). Stable carbon isotope composition falls within a narrow range along the shelf (-21.2‰ to -22.6‰), with inner shelf stations more isotopically depleted (average -22.5) than outer shelf sediments (average -21.7 ; see also Gordon et al., 2001). Slope sediments

have a similar isotopic composition, with observed values between -20.2‰ and -22.1‰ . The spatial pattern of $\delta^{13}\text{C}_{\text{OC}}$ could be interpreted as a dilution of terrigenous input at deeper regions of the study area. The most depleted $\delta^{13}\text{C}_{\text{OC}}$ values within the Mississippi slope are measured at the most distal station (2270 m), however, suggesting that dilution of terrigenous with marine sources at increasing distance from shore cannot entirely explain the spatial variability in isotopic composition.

Spatial variability in average lignin content (A , mg/100 mg OC) mirrors that observed for $\delta^{13}\text{C}_{\text{OC}}$ (Fig. 4). A is highest along the inner shelf, with an average value of 1.8 mg/100 mg OC. A of outer shelf sediments is slightly lower, with values ranging between 0.9 and 1.9 mg/100 mg OC. At the slope

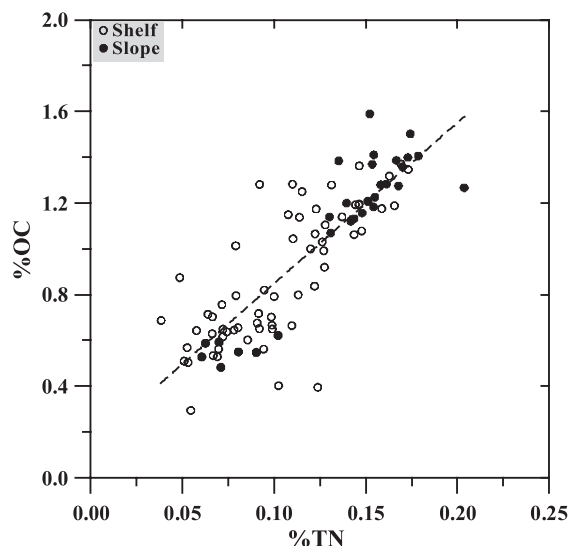


Fig. 5. Relationship between OC and TN for box core sediment samples. Sediment samples from shelf locations are indicated by open circles and samples from slope locations are indicated by closed circles. The linear regression based on all data points ($r^2=0.77$) is indicated by the dashed line.

stations, Δ is markedly lower than the shelf, with values that range between 0.2 and 0.6 mg/100 mg OC. Elevated levels of lignin on the inner shelf are consistent with the delivery of coarse terrigenous material to this region via the prevailing westward-flowing current, as well as with the small contribution from lignin-rich, isotopically depleted plant debris deposited at these sampling locations (Gordon and Goñi, 2003). Furthermore, while lignin-rich plant fragments are deposited relatively close to shore, soil-derived OM with a much lower lignin content and a more isotopically enriched signature is transported to deeper regions of the study area.

The observed enrichment in $\delta^{13}\text{C}_{\text{OC}}$ and coincident decrease in Δ with increasing water depth has traditionally been viewed as a simple dilution of a terrigenous with a marine OM source. Given the heterogeneity in the terrigenous OM source itself, an alternative explanation is that Δ decreases offshore due to preferential offshore transport of a low-lignin, soil-derived OM endmember (Goñi et al., 1998). The radiocarbon contents of surface sediments in the present study support this latter interpretation. The surface sediments throughout the study area are all characterized by depleted $\Delta^{14}\text{C}_{\text{OC}}$ values, ranging

between -203‰ and -452‰ (Table 2), indicating the significant presence of ‘old’ carbon. In addition, the radiocarbon content of sedimentary OM from the slope stations generally decreases with increasing water depth (Fig. 4), a trend that is opposite to that expected if increased fresh marine carbon were responsible for the enriched $\delta^{13}\text{C}_{\text{OC}}$. Instead, the observed trends in stable and radiocarbon isotope composition are more likely due to the offshore transport of old carbon with an enriched $\delta^{13}\text{C}$, such as soil-derived OM from the Mississippi drainage basin.

The lignin phenol compositions measured in this study provide further support for this interpretation (Fig. 6; Table 4). For example, significant increases are measured in the sedimentary acid to aldehyde (Ad/Al) ratios in both vanillyl (Vd/Vl) and syringyl (Sd/SI) phenols, and in 3,5-Bd/V ratios, with water depth. These parameters are thought to reflect the oxidative history of lignin (Hedges et al., 1988; Goñi et al., 1993). Ad/Al values greater than 0.4, and 3,5-Bd/V values greater than 0.1, are commonly observed in geochemical samples containing highly altered lignin, such as soils and highly decayed woods due to the activity of soft-rot and white-rot fungi (e.g., Hedges et al., 1988; Prahl et al., 1994). The spatial distribution of these parameters is consistent with the offshore transport and deposition of highly altered lignin remains, most likely associated with soil-derived fine clays exported by the Atchafalaya and Mississippi Rivers. Because these materials contain little recognizable lignin, such a physical sorting process also explains the drop in lignin accumulation observed between shelf and slope locations.

It is possible to argue that lignin may be degraded in situ during transport, thus explaining the high Ad/Al and 3,5-Bd/V ratios and low lignin contents of slope sediments. Subaqueous decay of plant tissues has been shown to increase Ad/Al ratios (Opsahl and Benner, 1995), as is observed during lignin degradation in terrestrial aerobic environments (Hedges et al., 1988). Oxidative lignin decay on land is also known to decrease the lignin phenol ratios S/V and C/V (Hedges et al., 1988; Hedges and Weliky, 1989), and a decrease in C/V has been observed during subaqueous lignin decay (Opsahl and Benner, 1995). Degradation of lignin on the inner shelf may be partly responsible for the lower deposition rate of lignin observed on the

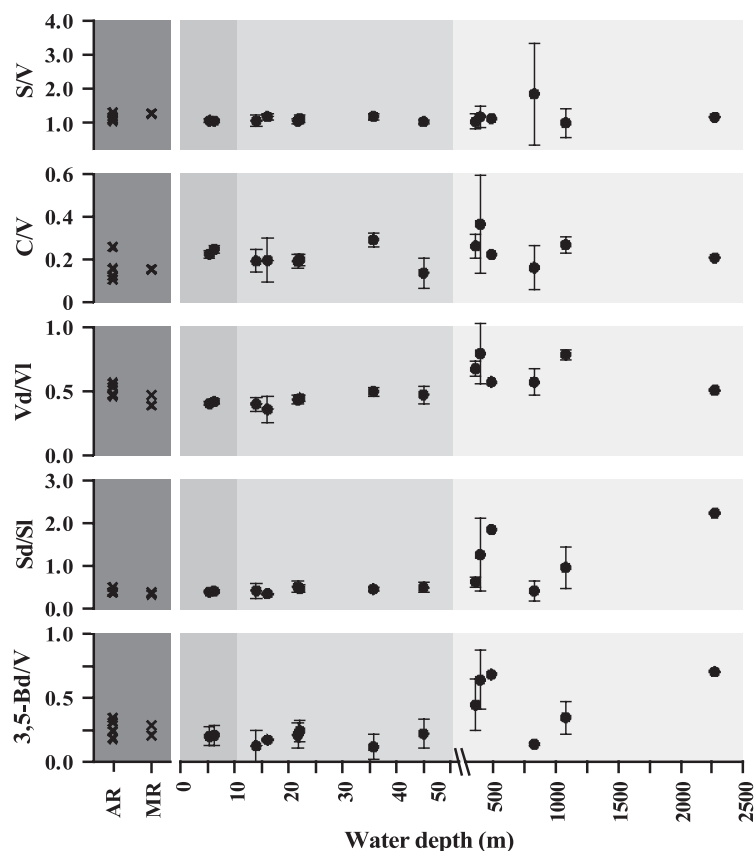


Fig. 6. Lignin composition of river suspended sediments and sediment synchrons from the study area. Different regions of the study area are indicated by the gray shading: river suspended sediments; inner shelf (<10 m water depth); outer shelf (10–200 m water depth); slope (>200 m water depth). S, sum of syringyl phenols, V, sum of vanillyl phenols; C, sum of cinammyl phenols; Vd, vanillic acid; Vl, vanillin; Sd, syringic acid; SI, syringaldehyde; 3,5-Bd, 3,5-dihydroxybenzoic acid.

outer shelf and slope (Fig. 3), particularly in light of the high turnover rates that characterize mobile mud belts (Aller, 1998). In situ degradation during offshore transit seems unlikely to be responsible for the observed spatial trend, however, given that there are no significant changes in the S/V and C/V ratios of sediment synchrons across the margin (Fig. 6; Table 4). In addition, by using sediment synchrons rather than surficial sediment intervals, lignin of similar age is being compared. Further, there are no measurable downcore changes in these lignin parameters that would suggest significant diagenetic alteration. The observed spatial trend in lignin compositional parameters is therefore best explained by the offshore transport of a degraded endmember, such as soil-derived OM.

3.3. Role of mineral surface area in organic matter distribution

The differential transport of mineral-associated OM appears to play an important role in determining the composition of sedimentary OM in the present study area. In order to examine such geological controls on bulk and terrigenous OM, we examine the relationship between surface area and OC and lignin contents in the sediments analyzed. Mineral surface area (SA) at the inner shelf stations ranges between 30 and 50 m²/g (Fig. 7a, Table 2) owing to the delivery of fine-grained material to the inner shelf via the Atchafalaya mud stream. The majority of outer shelf sediments are characterized by relatively low surface area values (15–25 m²/g), with the exception of the 36 m station

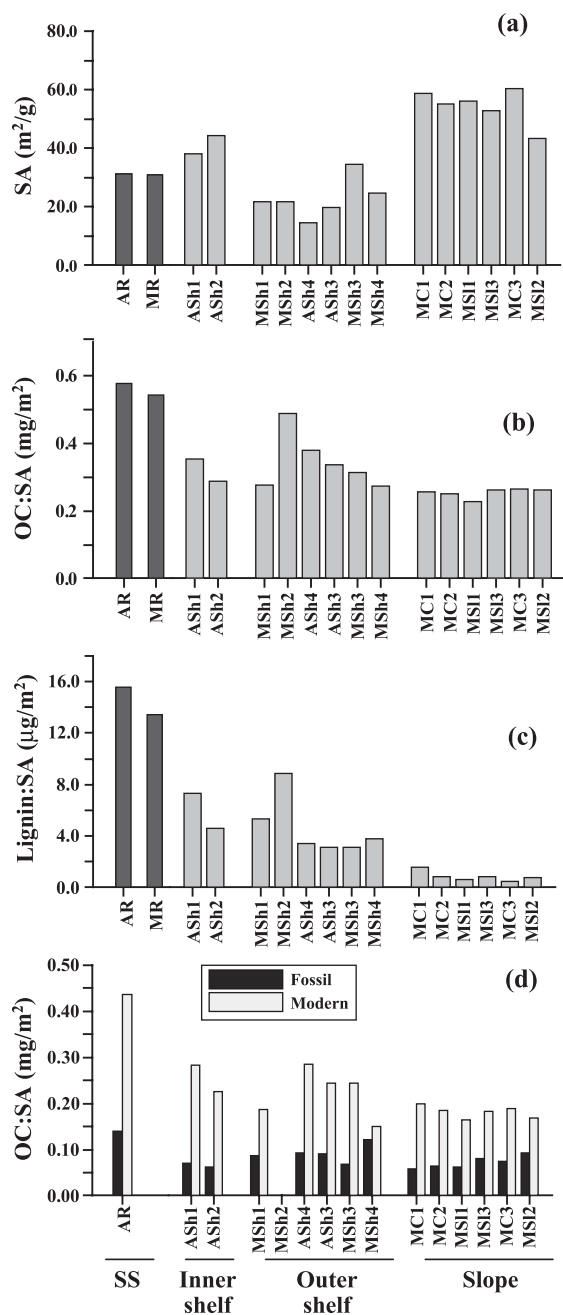


Fig. 7. (a) Mineral surface area, and (b) OC, (c) lignin, and (d) OC_{mod} and OC_{fos} loading of sediment particles. Surface area and loadings are shown for river suspended sediments (SS) and surface sediments from each box core location, indicated on the x-axis. Modern and fossil carbon fractions calculated based on fraction modern (F_m ; Table 2). River SS data from Gordon and Goñi (2003).

(34 m²/g). The highest surface area values from the study area are observed in slope sediments, with values ranging from 43 to 60 m²/g. The higher mineral SA values in the slope versus the shelf are likely due to the hydrodynamic sorting that occurs during cross-margin sediment transport and the deposition of increasingly finer clastic materials (i.e., land-derived clays) at the offshore locations. That the lowest SA for the slope sediments was observed at the most distal location (MSI2) may be due to the enhanced inputs of relatively coarse biogenic particles with water depth, as illustrated by the increases in the CaCO₃ content of sediments from ~3% in the shelf to >10% (maximum of 24% at MSI2) in the slope (Table 2).

A significant linear correlation exists between OC and SA ($r^2=0.81$, Fig. 8), indicating that association of OM with mineral surfaces (both clastic and biogenic) exerts an important control over the measured OM content in the Mississippi shelf and slope, as was observed for the Atchafalaya shelf (Gordon et al., 2001). The surface area loading of OC for the majority of the sediments deposited in the

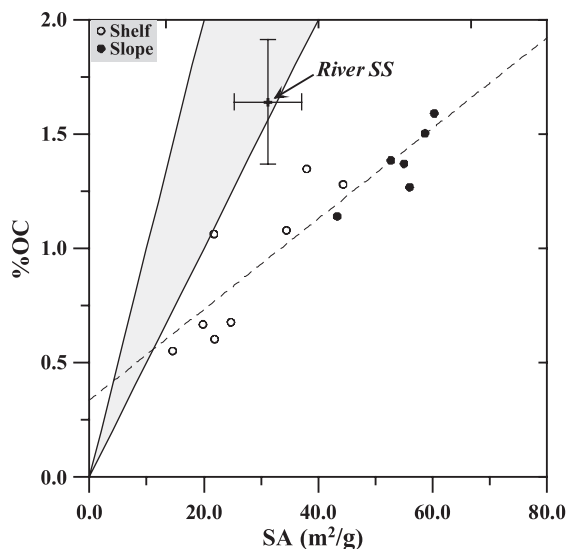


Fig. 8. Relationship between OC and SA. Sediment samples from shelf locations are indicated by the open circles and samples from slope locations are indicated by closed circles. The range of values for river suspended sediments (SS), indicated by the solid lines, are calculated as one standard deviation about the mean of values reported in Gordon and Goñi (2003). The linear relationship between OC and SA ($r^2=0.81$) is indicated by the dashed line. The typical range observed for marine sediments (0.5–1.0 mgC/m²; Mayer, 1994; Hedges and Keil, 1995) is indicated by the shaded region.

study area is lower than is typical of marine sediments (Fig. 8; 0.5–1.0 mg/m²; Mayer, 1994; Hedges and Keil, 1995). Low OC loadings have previously been observed in deltaic sediments, which was explained by the loss of >70% of riverine carbon upon delivery to the coastal ocean (Keil et al., 1997). The authors further suggested that carbon derived from autochthonous sources partially reloaded these particles based on the relative isotopic enrichment of deltaic versus river sediments. Although a similar loss and replacement scenario may explain the low OC/SA loadings and $\delta^{13}\text{C}_{\text{OC}}$ enrichment of sediments from the Mississippi/Atchafalaya shelf relative to those in suspended river particles, this explanation is not consistent with the $\Delta^{14}\text{C}_{\text{OC}}$ data. Instead, the physical sorting of particles that occurs in the inner coastal margin provides an alternative explanation to the observed trends. For example, deposition of discrete coarse plant material in delta regions also contributes to the decrease in OC/SA ratios by sequestering land-derived, OC-rich materials in the sediments immediately adjacent to river mouths. Mineral loadings of bulk OC, lignin, modern carbon, and fossil carbon may help evaluate the relative importance of loss and replacement versus physical sorting on the composition of sedimentary OM in the present study area. OC loadings of inner shelf sediments (average 0.32 mg C/m²) are lower than river SS (average 0.55 mg C/m²), indicating a loss of riverine carbon from particles (Fig. 7b). The OC loadings of outer shelf sediments (average 0.34 mg C/m²) are not significantly different from those on the inner shelf. The major exception is the relatively high OC/SA values measured in the MSh2 and ASh4 samples (Fig. 7b). The addition of marine carbon to sediments from these locations may explain the greater OC loadings than those measured in the inner shelf, where autochthonous production is likely limited due to turbidity (Sklar and Turner, 1981). Beyond the shelf break, the OC loadings remain relatively constant at 0.25 mg C/m² over a wide range of water depths (365–2270 m).

Unlike OC, there is no significant correlation between lignin content and mineral SA ($r^2=0.24$). The lack of such a relationship with lignin underscores the heterogeneous composition of lignin-bearing material delivered to and deposited in the study area (Gordon and Goñi, 2003). The surface area-normalized lignin content shows a remarkable

decrease in lignin loading from river suspended sediments (15.4 $\mu\text{g}/\text{m}^2$) to those deposited on the inner shelf (average 6.0 $\mu\text{g}/\text{m}^2$) (Fig. 7c). These trends are consistent with rapid loss of lignin-bearing terrigenous carbon upon its delivery to the coastal ocean. However, this apparent loss is likely due to the preferential deposition of discrete plant fragments, which are higher in lignin and not tightly associated with mineral grains, in the deltaic regions adjacent to river mouths. Further study of deltaic sediments should provide more details and insight on such a lignin loss term.

Lignin loadings in the outer shelf (average 4.6 $\mu\text{g}/\text{m}^2$) are slightly lower than those of the inner shelf and are relatively constant with the exception of the MSh2 station, which also showed a higher bulk OC loading (Fig. 7). The SA-normalized lignin contents of slope surface sediments (average 0.8 $\mu\text{g}/\text{m}^2$) are markedly lower than those on the shelf. Such a trend suggests that lignin-bearing OM is removed from particles during offshore transit to the slope. One possibility is that lignin is degraded preferentially to other forms of carbon as materials move from shelf to slope. A more likely explanation, however, is that the hydrodynamic sorting that occurs during cross-shelf transport preferentially mobilizes lignin-poor fine particles, such as soil-derived fine clays. The addition of mineral surfaces from biogenic sediment sources that contain no lignin, such as calcite tests from planktonic and benthic organisms, is another way in which lignin:SA ratios may be lowered. However, it is not clear if the large decreases in lignin loadings between shelf and slope sediments (from ca. 4 to <1 $\mu\text{g}/\text{m}^2$, respectively) can be explained by relatively moderate increases in CaCO₃ content measured at these locations (ca. 4% in the shelf, 10–20% in the slope). A more detailed study of the contributions from biogenic sediments to the overall mineral surface area is needed to better assess this effect.

Relative loadings of modern ($\text{OC}_{\text{mod}}=\%\text{OC}\cdot F_{\text{m}}$) and fossil ($\text{OC}_{\text{fos}}=\%\text{OC}\cdot(1-F_{\text{m}})$) carbon onto mineral particles (Fig. 7d) provide additional constraints on processes that control the distribution of OM in the present study area. The OC_{mod} loading of all surficial sediments is lower than that observed in river SS, and shows a general decrease with water depth in deeper regions (between 20 and 2000 m water depth). The high OC_{mod} loading observed in river SS (Fig. 7d),

due to the presence of modern terrigenous material, is likely in the form of coarse plant fragments. Rapid deposition from the river load of these discrete plant fragments upon delivery to the coast is indicated by lower observed OC_{mod} loadings of shelf sediments. Higher modern carbon loadings observed at several outer shelf locations (ca. 20 m water depth) may be due to the addition of marine-derived OM to particles. This is consistent with the observation that the highest rates of primary productivity in surface waters of the northern Gulf of Mexico occur at intermediate salinities of 20–30 (Lohrenz et al., 1999), values that coincide with the outer shelf region of the present study. Subsequent loss of this labile carbon pool is likely responsible for the decrease in OC_{mod} loadings of slope sediments.

Fossil carbon, on the other hand, exhibits a relatively constant loading throughout the wide range of water depths, consistent with nearly conservative transport and deposition of this OM pool across the northern Gulf of Mexico margin. There is a slight increase in fossil carbon loading from the head of the Mississippi Canyon (MC1) to the most distal slope station (MS12). The observed OC_{fos}/SA increase suggests that finer particles that are delivered to the deeper regions of the study area are enriched in an ‘old’ carbon pool. This result provides additional evidence that the compositional character of sediments from the study area is primarily controlled by offshore export of fine clastic material that is composed of compositionally distinct terrigenous carbon. The radiocarbon composition of the lignin biomarkers would provide further evidence for such a scenario.

4. Summary and conclusions

The fate of terrigenous OM in the ocean has historically been described by rapid loss of compositionally homogenous plant-derived material seaward of river mouths and its subsequent dilution with marine carbon (e.g., Hedges and Parker, 1976; Hedges and Mann, 1979). More recent evidence suggests that delivery and quantification of terrigenous OM in margin sediments is complicated by the heterogeneous nature of the riverine endmember (e.g., Hedges et al., 1986; Prahl et al., 1994; Goñi et al., 1998; Gordon and Goñi, 2003). The fate of terrigenous OM

in the northern Gulf of Mexico appears to be governed by hydrodynamic sorting of riverine particles of different compositional character rather than by simple dilution with marine OM. We propose that a fraction of the riverine particles are comprised of plant fragments and sediments that contain a modern $\Delta^{14}C_{\text{OC}}$ signature and a depleted $\delta^{13}C_{\text{OC}}$, indicative of modern, C3 vascular plants. Prior observations suggest that much of this material is rapidly deposited within the main river channel (Bianchi et al., 2002) or close to shore (Gordon and Goñi, 2003), as evidenced by the elevated lignin accumulation rates on the inner shelf and the decreases in both OC_{mod}/SA and lignin:SA ratios between the river SS and the shelf sediments. This process is responsible for the disproportionate deposition of OM and lignin in the inner Atchafalaya shelf region. The high sedimentation rates and elevated OC and lignin contents of two cores from the inner shelf west of the Mississippi River delta (Eadie et al., 1994) suggest that a similar process occurs in this region.

As sediments move along the dispersal system, the finer particle fraction is preferentially transported along and across the margin to distal regions of the study area. Our data indicate that this fraction is mainly composed of soil-derived OM. This aged, land-derived OM pool is characterized by a lower lignin content and an enriched $\delta^{13}C_{\text{OC}}$. The OM on the outer shelf, which accumulates at a lower rate than on the inner shelf, appears to contain both marine and terrigenous OM sources. This is indicated by the apparent ‘addition’ of a modern carbon source to particles prior to deposition in this region and the observed spatial distribution of primary productivity in the study area (Lohrenz et al., 1999), which is highest at intermediate salinities.

The export of particle-associated OM from the coastal ocean (<200 m) to the slope region is indicated by relatively high OC accumulation rates (33% of the total OC for the study area), but lower overall OC/SA ratios. The lignin-bearing material that accumulates in this deep region is compositionally distinct from terrigenous OM that is deposited on the shelf given the lower observed levels of lignin and difference in lignin compositional parameters. The material that accumulates in this region appears to be composed of a significant fraction of old carbon, consistent with a soil-derived OM input. Further characterization of

terrigenous OM from these sediments using compound-specific ^{13}C and ^{14}C isotope analysis is needed to quantitatively understand the ultimate fate of this material in ocean margins.

Acknowledgements

We thank Gail Kineke for ship time, which was supported by the Office of Naval Research Award #NOOO14-98-1-0083. We thank the captain and crew of the R/V Pelican, as well as M. Teixeira, C. Jones, R. Potter, D. Hartz, D. Perkey, S. Murphy, and K. Peterson for help with sample collection. M. Allison conducted the ^{210}Pb measurements, and is acknowledged along with W. Moore for detailed discussions of the accumulation rate data. We thank H. Aceves, and E. Tappa for help with elemental and isotope analyses. M. Cathey, M. Woodworth, F. Prah, and one anonymous reviewer are thanked for valuable comments on the manuscript. This research was funded by National Science Foundation grant OCE-9711822 to M. Goñi and a NSF Graduate Fellowship and EPA STAR Fellowship to E. Gordon.

References

- Aller, R.C., 1998. Mobile deltaic and continental shelf muds as suboxic, fluidized bed reactors. *Mar. Chem.* 61, 143–155.
- Allison, M.A., Kineke, G.C., Gordon, E.S., Goñi, M.A., 2000. Development and reworking of a seasonal flood deposit on the inner continental shelf off the Atchafalaya river. *Cont. Shelf Res.* 20, 2267–2294.
- Berner, R.A., 1982. Burial of organic carbon and pyrite sulfur in the modern ocean: its geochemical and environmental significance. *Am. J. Sci.* 282, 451–473.
- Berner, R.A., 1989. Biogeochemical cycles of carbon and sulfur and their effect on atmospheric oxygen over phanerozoic time. *Palaeogeogr. Palaeoclimatol. Palaeoecol.* 75, 97–122.
- Bianchi, T.S., Lambert, C.D., Santschi, P.H., Guo, L., 1997. Sources and transport of land-derived particulate and dissolved organic matter in the gulf of Mexico (Texas shelf/slope): the use of lignin-phenols and loliolides as biomarkers. *Org. Geochem.* 27, 65–78.
- Bianchi, T.S., Mitra, S., McKee, B.A., 2002. Sources of terrestrially derived organic carbon in lower Mississippi river and Louisiana shelf sediments: implications for differential sedimentation and transport at the coastal margin. *Mar. Chem.* 77, 211–223.
- Brunauer, S., Emmett, P.H., Teller, E., 1938. Adsorption of gases in multimolecular layers. *J. Am. Chem. Soc.* 60, 309–319.
- de Haas, H., van Weering, T.C.E., de Stigter, H., 2002. Organic carbon in shelf seas: sinks or sources, processes, and products. *Cont. Shelf Res.* 22, 691–717.
- Eadie, B.J., McKee, B.A., Lansing, M.B., Robbins, J.A., Metz, S., Treftly, J.H., 1994. Records of nutrient-enhanced coastal ocean productivity in sediments from the Louisiana continental shelf. *Estuaries* 17, 754–765.
- Gearing, P., Plucker, F.E., Parker, P.L., 1977. Organic carbon stable isotope ratios of continental margin sediments. *Mar. Chem.* 5, 251–266.
- Goñi, M.A., Montgomery, S., 2000. Alkaline CuO oxidation with a microwave digestion system: lignin analyses of geochemical samples. *Anal. Chem.* 72, 3116–3121.
- Goñi, M.A., Thomas, K.A., 2000. Sources and transformations of organic matter in surface soils and sediments from a tidal estuary (north inlet South Carolina, USA). *Estuaries* 23, 548–564.
- Goñi, M.A., Nelson, B., Blanchette, R.A., Hedges, J.I., 1993. Fungal degradation of wood lignins—geochemical perspectives from CuO-derived phenolic dimers and monomers. *Geochim. Cosmochim. Acta* 57, 3985–4002.
- Goñi, M.A., Ruttenger, K.C., Eglinton, T.I., 1997. Sources and contribution of terrigenous organic carbon to surface sediments in the gulf of Mexico. *Nature* 389, 275–278.
- Goñi, M.A., Ruttenger, K.C., Eglinton, T.I., 1998. A reassessment of the sources and importance of land-derived organic matter in surface sediments from the gulf of Mexico. *Geochim. Cosmochim. Acta* 62, 3055–3075.
- Gordon, E.S., Goñi, M.A., 2003. Sources and distribution of terrigenous organic matter delivered by the Atchafalaya river to sediments in the northern gulf of Mexico. *Geochim. Cosmochim. Acta* 67, 2359–2375.
- Gordon, E.S., Goñi, M.A., Roberts, Q.N., Kineke, G.C., Allison, M.A., 2001. Organic matter distribution and accumulation on the inner Louisiana shelf west of the Atchafalaya river. *Cont. Shelf Res.* 21, 1691–1721.
- Hedges, J.I., 1992. Global biogeochemical cycles—progress and problems. *Mar. Chem.* 39, 67–93.
- Hedges, J.I., Keil, R.G., 1995. Sedimentary organic matter preservation: an assessment and speculative synthesis. *Mar. Chem.* 49, 81–115.
- Hedges, J.I., Mann, D.C., 1979. The lignin geochemistry of marine sediments from the southern Washington coast. *Geochim. Cosmochim. Acta* 43, 1809–1818.
- Hedges, J.I., Parker, P.L., 1976. Land-derived organic matter in surface sediments from the gulf of Mexico. *Geochim. Cosmochim. Acta* 40, 1019–1029.
- Hedges, J.I., Stern, J.H., 1984. Carbon and nitrogen determinations of carbonate containing solids. *Limnol. Oceanogr.* 49, 657–663.
- Hedges, J.I., Weliky, K., 1989. Diagenesis of conifer needles in a coastal marine environment. *Geochim. Cosmochim. Acta* 53, 1–15.
- Hedges, J.I., Clark, W.A., Quay, P.D., Richey, J.E., Devol, A.H., Santos, U.M., 1986. Composition and fluxes of particulate organic material in the Amazon river. *Limnol. Oceanogr.* 31, 717–738.

- Hedges, J.I., Blanchette, R.A., Weliky, K., Devol, A.H., 1988. Effects of fungal degradation on the CuO oxidation products of lignin—a controlled laboratory study. *Geochim. Cosmochim. Acta* 52, 2717–2726.
- Hedges, J.I., Keil, R.G., Benner, R., 1997. What happens to terrestrial organic matter in the ocean? *Org. Geochem.* 27, 195–212.
- Keil, R.G., Mayer, L.M., Quay, P.D., Richey, J.E., Hedges, J.I., 1997. Loss of organic matter from riverine particles in deltas. *Geochim. Cosmochim. Acta* 61, 1507–1511.
- Lohrenz, S.E., Fahnenstiel, G.L., Redalje, D.G., Lang, G.A., Dagg, M.J., Whitedge, T.E., Dortch, Q., 1999. Nutrients, irradiance, and mixing as factors regulating primary production in coastal waters impacted by the Mississippi river plume. *Cont. Shelf Res.* 19, 1113–1141.
- Mayer, L.M., 1994. Surface area control of organic carbon accumulation in continental shelf sediments. *Geochim. Cosmochim. Acta* 58, 1271–1284.
- McNichol, A.P., Gagnon, A.R., Jones, G.A., Osborne, E.A., 1992. Illumination of a black box: analysis of gas composition during graphite target preparation. *Radiocarbon* 34, 321–329.
- Milliman, J.D., Meade, R.H., 1983. World-wide delivery of river sediment to the ocean. *J. Geol.* 91, 1–21.
- Nittrouer, C.A., Sternberg, R.W., Carpenter, R., Bennett, J.T., 1979. The use of Pb-210 geochronology as a sedimentological tool: application to the Washington continental shelf. *Mar. Geol.* 31, 297–316.
- Opsahl, S., Benner, R., 1995. Early diagenesis of vascular plant tissues: lignin and cutin decomposition and biogeochemical implications. *Geochim. Cosmochim. Acta* 59, 4889–4904.
- Pakulski, J.D., Benner, R., Whitedge, T., Amon, R., Eadie, B., Cifuentes, L., Ammerman, J., Stockwell, D., 2000. Microbial metabolism and nutrient cycling in the Mississippi and Atchafalaya river plumes. *Estuar. Coast. Shelf Sci.* 50, 173–184.
- Parton, W.J., Schimel, D.S., Cole, C.V., Ojima, D.S., 1987. Analysis of factors controlling soil organic matter levels in great plains grasslands. *Soil Sci. Soc. Am. J.* 51, 1173–1179.
- Penland, S., Ramsey, K.E., 1990. Relative sea-level rise in Louisiana and the gulf of Mexico—1908–1988. *J. Coast. Res.* 6, 323–342.
- Prahl, F.G., Ertel, J.R., Goñi, M.A., Sparrow, M.A., Eversmeyer, B., 1994. Terrestrial organic carbon contributions to sediments on the Washington margin. *Geochim. Cosmochim. Acta* 58, 3035–3048.
- Premuzic, E.T., Benkovitz, C.M., Gaffney, J.S., Walsh, J.J., 1982. The nature and distribution of organic matter in the surface sediments of world oceans and seas. *Org. Geochem.* 4, 63–77.
- Rabalais, N.N., Turner, R.E., Justic, D., Dortch, Q., Wiseman Jr., W.J., 1999. Characterization of hypoxia: Topic 1. Report for the Integrated Assessment of Hypoxia in the Gulf of Mexico, NOAA Coastal Ocean Program Decision Analysis Series, vol. 16. NOAA Coastal Ocean Program, Silver Springs, MD. 167 pp.
- Redfield, A.C., Ketchum, B.H., Richards, F.A., 1963. The influence of organisms on the composition of seawater. In: Hill, M.N. (Ed.), *The Sea*, vol. 2. John Wiley and Sons, New York, pp. 26–77.
- Sackett, W.M., Thompson, R.R., 1963. Isotopic organic carbon composition of recent continental derived clastic sediments of eastern gulf coast, gulf of Mexico. *Am. Assoc. Pet. Geol. Bull.* 47, 525–531.
- Sklar, F.H., Turner, R.E., 1981. Characteristics of phytoplankton production off Barataria bay in an area influenced by the Mississippi river. *Contrib. Mar. Sci.* 24, 93–106.
- Stuiver, M., Polach, H.A., 1977. Discussion: reporting of ¹⁴C data. *Radiocarbon* 19, 355–363.
- Taylor, J.R., 1982. *An Introduction to Error Analysis: The Study of Uncertainties in Physical Measurements*. University Science Books, Mill Valley, CA.
- Tiessen, J., Stewart, J.W.B., Hunt, H.W., 1984. Concepts of soil organic matter transformation in relation to organo-mineral particle size fractions. *Plant Soil* 76, 287–295.
- Velasco, D.W., 2003. Shallow stratigraphy observations using electrical resistivity and dual-frequency echosounding methods. MS thesis, Boston College, Boston, MA.
- Vogel, J.J., Southen, J.R., Nelson, D.E., 1987. Catalyst and binder effects in the use of filamentous graphite for AMS. *Nucl. Instrum. Methods Res., B* 29, 50–56.
- Wells, J.T., Kemp, G.P., 1981. Atchafalaya mud stream and recent mudflat progradation: Louisiana chenier plain. *Trans.-Gulf Coast Assoc. Geol. Soc.* 31, 409–416.
- U.S. Army, Corps of Engineers, 1974. Deep Draft Access to the Ports of New Orleans and Baton Rouge. Draft Environmental Statement. Corps of Engineers, New Orleans District.